Progress In Electromagnetics Research, PIER 61, 231–252, 2006

A NOVEL MODELING TECHNIQUE TO SOLVE A CLASS OF RECTANGULAR WAVEGUIDE BASED CIRCUITS AND RADIATORS

S. Das and A. Chakrabarty

Department of Electronics and Electrical Communication Engineering
Indian Institute of Technology - Kharagpur
West Midnapore, West Bengal, PIN-721302, India

Abstract—A new methodology has been developed, based on moment method; for analyzing a class of rectangular waveguide based circuits and radiators. The methodology involves in modeling the given structure using tetragonal bricks or cavities and then replacing all the apertures and discontinuities with equivalent magnetic current densities so that the given structure can be analyzed using only the Magnetic Field Integral Equation (MFIE). As it is necessary to use a number of such cavities in order to study these complicated waveguide structures, the present method is named as Multiple Cavity Modeling Technique (MCMT). The major advantage for using the MCMT in rectangular waveguide based structures is the fact that since only the magnetic currents present in the apertures are considered the methodology involves only solving simple magnetic field integral equations rather the coupled integral equation involving both the electric and magnetic currents. Further it is possible to consider both co and cross polarization and also the thickness of the waveguide discontinuities like diaphragm thickness or window thickness in the analysis. Due to this, it is possible to get highly accurate result. It is also possible to extend the method to any number of resonators, cavities or irises regardless of the polarization.

To demonstrate, the methodology has been applied to analyze an open end of a waveguide with dielectric plug, both in transmitting and receiving mode, and a waveguide step discontinuity. Even mode and odd mode admittances of interacting identical inductive diaphragms have also been calculated using this methodology. Data obtained using this technique has been compared with measured, CST microwave studio simulation and literature available data. The theory has been validated by the reasonable agreement obtained between experimental data, simulated data and literature available data with numerical data.

1. INTRODUCTION

With increasing importance of waveguide based antennas in radar, satellite and mobile communication systems the theoretical studies on these topics have occupied the interests of numerous researchers for several decades. The number of research work in this area is extremely large that a general overview itself will be a report of its own. Gupta, Bhattacharyya and Chakraborty [1] analyzed an open ended waveguide radiator with dielectric plug using stub waveguide technique. This analysis demonstrates that such a structure behaves as a very good radiator of microwave energy over a band of frequencies. The analysis also shows that the frequency band of best match can be varied over the frequency by adjusting the thickness of the plug which is inserted at the radiating end. Calvin T. Swift [2, 3] calculated the admittance of a rectangular aperture antenna loaded with a dielectric plug as a boundary value problem. Katirch, Dumin and Dumina [4] solved the problem of excitation of rectangular waveguide by transient current in time domain by the evolutionary equation technique and the Riemann function method. The field radiated from the open end of the rectangular waveguide was calculated in Kirchoff's approximation using vector potential method. Multiple cavity modeling technique (MCMT) [5, 6], modal and hybrid modal spectral technique [7], transverse operator method [8], extrapolation technique [9], variational method [10, 11], co-relation matrix method [12] and moment method [13] also has been used to compute the aperture admittance or reflection coefficient of an open-ended or window loaded waveguide radiator with infinite flange.

The waveguide junction is the building block of many microwave components and the scattering characteristics of different waveguide junction have already been studied by many researchers in the past. Some important properties for the generalized scattering matrix of waveguide step discontinuities, in the context of the mode matching technique, are derived in [14] by considering the conservation of the complex power and self reaction across the discontinuities. Mongiardo et al. [15] considered the problem of waveguide step discontinuity from the perspective of generalized network formulation. In [16] an H-plane waveguide component with arbitrary shape is analyzed using finite element technique in conjunction with boundary element method (BEM). For the application of BEM in the waveguide structure, a ray representation of the waveguide Green's function is used. Lin et al. [17] proposed a unified mode matching technique (MMT) for the calculation of the modal scattering matrix of concentric waveguide junctions. The TE and TM modal fields in both waveguides which

are connected to form the junction are expressed in the Cartesian coordinate system, so that the coupling coefficients for all the modes can be evaluated effectively. Wexler presented a solution of waveguide discontinuities by modal analysis [18]. In this method, the amplitudes of normal modes are chosen so as to satisfy the boundary conditions at the discontinuity. In [19] Leavy gave a derivation of equivalent circuits of microwave structures using numerical techniques. One of the objectives of this paper was to advocate the derivation of equivalent circuits rather than leaving solutions of microwave network problems as a collection of numerical data. Guglielmi and Newport [20] presented a rigorous, multimode equivalent network representation of inductive discontinuities. However the thickness of the irises was not included in this paper.

Perhaps the most important circuit among the waveguide junction based structures is the waveguide irises. The necessity of finding an exact equivalent network representation for the inductive irises having finite thickness and interacting via higher order modes arises in the design of high-precision waveguide filter. The interaction of two infinitely thin inductive irises has been discussed by Palais [21] employing an "obstacle" formulation. In [22] Schwinger function has been assumed for the trial field. This allows the solution of the infinitely thin irises to be used directly in conjunction with the equivalent network representation of the thick iris. Rozzi also applied variational method [23] to analyze thick rectangular irises. The analysis involves both the Eigen mode and Schwinger expansion on the aperture. The variational approach to the problem of one isolated iris also has been studied by Collin [24].

In this paper a new technique based on moment method [25, 26], named Multiple Cavity Modeling Technique, has been described for analyzing a class of waveguide aperture antennas and devices. The technique involves in replacing all the apertures and discontinuities of the rectangular waveguide based structures, with equivalent magnetic current densities so that the given structure can be analyzed using only Magnetic Field Integral Equation (MFIE). To make the MFIE applicable to the generalized waveguide structures problem, the given structure is modeled using rectangular cavities. As it is necessary to use a number of such cavities in order to study these complicated waveguide structures, the present method is named as Multiple Cavity Modeling Technique (MCMT). The interfacing apertures between different regions (waveguide-cavity, cavity-cavity, cavity-half space) are then replaced by equivalent magnetic current densities. The magnetic field scattered inside the cavity region due to this source is determined by using cavity Green's function of the electric vector potential. The

cavity Green's function has been derived by solving the Helmholtz equation for the electric vector potential for unit magnetic current source. The scattered magnetic field in the waveguide region due to the presence of transverse magnetic current densities is solved by rigorous mode matching method. By applying the continuity condition of the tangential magnetic field at the interfacing apertures, and expanding the unknown magnetic current densities in terms of entire domain sinusoidal basis function by using the Galerkin's specialization of Method of Moments, the problem is reduced to solving the simultaneous linear equation from which the co-efficients of the basis function representing the aperture field are evaluated. Reflection and transmission coefficient seen by the feed waveguide and other arms are in terms of these co-efficients.

At the beginning, the methodology has been applied to analyze a dielectric plugged open ended waveguide in an infinite ground plane, which is basically an antenna, both in transmitting and receiving mode. MCMT has also been applied to study the classical problem of waveguide step discontinuity. A further configuration, which has been treated by this method, is the equivalent network for interacting identical thick inductive irises.

2. PROBLEM FORMULATION

2.1. Analysis of Open End of a Waveguide with Dielectric Plug in Transmitting and Receiving Mode Using MCMT

A developed Y-Z plane cross sectional view of the open end of a waveguide with finite thickness of the dielectric plug is shown in Figure 1 for transmitting mode. Figure 2 shows the same for receiving mode.

From the Figure 1 and Figure 2 it may be noted that the structures have three regions, namely, one waveguide region, one cavity region and one half space region. The interfacing apertures between different regions (waveguide-cavity, cavity-half space) are replaced by equivalent magnetic current densities. The magnetic current distribution in aperture 1 is M_x^1 whereas M_x^2 is the magnetic current distribution in aperture 2. The tangential components of magnetic fields in the three regions are as follows

Region 1:

$$2H_x^{inc} + H_x^{\text{int}}\left(-M_x^1\right) \qquad \text{(For transmitting mode)} \tag{1a}$$

$$H_x^{\text{int}}\left(-M_x^1\right) \qquad \text{(For receiving mode)} \tag{1b}$$

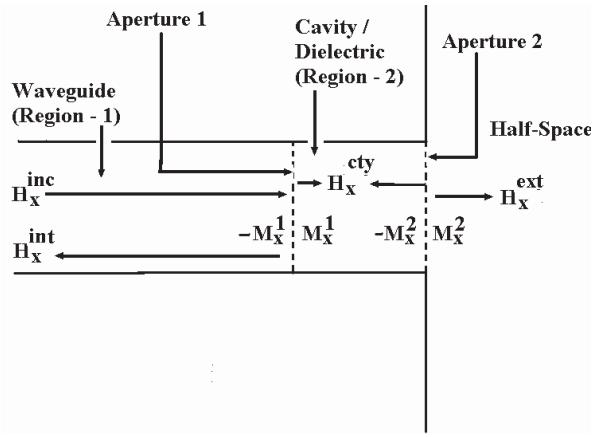

Figure 1. Cross-sectional view of an open end of waveguide with dielectric plug for transmitting mode.

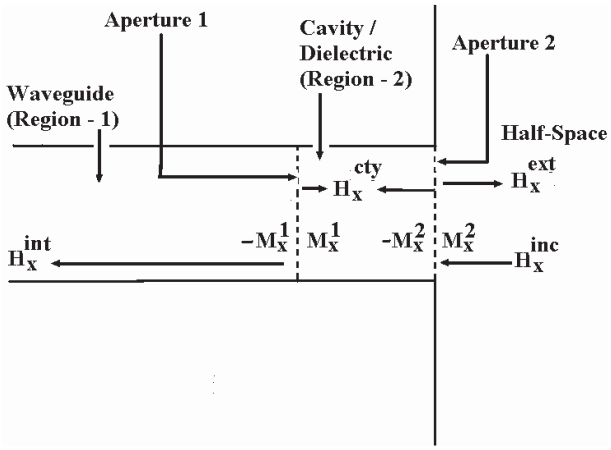

Figure 2. Cross-sectional view of an open end of waveguide with dielectric plug for receiving mode.

Region 2:

$$H_x^{cty}\left(M_x^1\right) + H_x^{cty}\left(-M_x^2\right) \tag{2}$$

Region 3:

$$H_x^{ext}\left(M_x^2\right) \qquad \text{(For transmitting mode)} \tag{3a}$$

$$H_x^{ext}\left(M_x^2\right) + 2H_x^{inc} \qquad \text{(For receiving mode)} \tag{3b}$$

It may be noted that we have neglected the existence of cross-polarization components in the analysis as cross-polarization components do not exist in rectangular waveguide. Applying the continuity of the tangential component of the magnetic field across the aperture 1 and aperture 2 we get the boundary conditions from equations (1)–(3) respectively as

For transmitting mode:

$$H_x^{\text{int}}\left(M_x^1\right) + H_x^{cty}\left(M_x^1\right) - H_x^{cty}\left(M_x^2\right) = 2H_x^{inc} \tag{4a}$$

$$-H_x^{cty}\left(M_x^1\right) + H_x^{cty}\left(M_x^2\right) + H_x^{ext}\left(M_x^2\right) = 0 \tag{4b}$$

For receiving mode:

$$H_x^{\text{int}}\left(M_x^1\right) + H_x^{cty}\left(M_x^1\right) - H_x^{cty}\left(M_x^2\right) = 0 \tag{5a}$$

$$-H_x^{cty}\left(M_x^1\right) + H_x^{cty}\left(M_x^2\right) + H_x^{ext}\left(M_x^2\right) = -2H_x^{inc} \tag{5b}$$

The magnetic currents at the apertures are assumed to be

$$M_x^{aperture} = \sum_{p=1}^{\infty} A_{px}^{aperture} m_{px}^{aperture} \tag{6}$$

where $A_{px}^{aperture}$ are basis coefficients and the basis function $m_{px}^{aperture}$ $(p = 1, 2, 3 \ldots M)$ are defined by

$$m_{px}^{aperture} = \begin{cases} \sin\left\{\dfrac{p\pi}{2a}(x-a)\right\} & \begin{matrix} -a \le x \le a \\ -b \le y \le b \end{matrix} \\ 0 & \text{elsewhere} \end{cases} \tag{7}$$

Where $2a \times 2b$ is the cross sectional dimension of the waveguide.

The X-component of incident magnetic field at the aperture 1 for transmitting mode is the dominant TE_{10} mode and is given by

$$H_x^{inc} = -Y_0 \cos\left(\frac{\pi x}{2a}\right) e^{-j\beta z} \tag{8}$$

whereas the X-component of incident magnetic field at the aperture 2, for receiving mode, is the plane wave and is given by

$$H_x^{inc} = \frac{1}{\eta} e^{-jk_z z} \tag{9}$$

Y_0 is the dominant mode characteristic admittance and is given by

$$Y_0 = \frac{1}{k\eta}\sqrt{k^2 - \left(\frac{\pi}{2a}\right)^2} \tag{10}$$

The tangential component of the magnetic field scattered inside the cavity is given by

$$H_x^{cty}(M_x) = \begin{cases} \dfrac{j\omega\varepsilon}{k^2}\displaystyle\sum_m \sin\left\{\frac{m\pi}{2a}(x+a)\right\}\cot\{2\Gamma_{m0}t\} \\ \qquad\qquad \text{if } m = p \text{ and } n = 0 \\ 0 \qquad\qquad \text{elsewhere} \end{cases} \tag{11}$$

where $2t$ is the thickness of the dielectric plug.

The magnetic field scattered inside the cavity region due to the source is determined by using cavity Green's function of the electric vector potential. The cavity Green's function has been derived by solving the Helmholtz equation for the electric vector potential for the unit magnetic current source. The Green's function for the cavity, shown in Figure 3, is given by

$$\begin{aligned} \tilde{G} \;=\; & \sum_{m=0}^{\infty}\sum_{n=0}^{\infty}\frac{\varepsilon_m\varepsilon_n}{4lw}\left[\hat{x}\hat{x}\cdot\sin\left\{\frac{m\pi}{2a}(x+a)\right\}\sin\left\{\frac{m\pi}{2a}(x_0+a)\right\}\right. \\ & \times\cos\left\{\frac{n\pi}{2b}(y+b)\right\}\cos\left\{\frac{n\pi}{2b}(y_0+b)\right\} \\ & \times\begin{cases}\cos\{\Gamma_{mn}(z-t)\}\cos\{\Gamma_{mn}(z_0+t)\} & z>z_0 \\ \cos\{\Gamma_{mn}(z_0-t)\}\cos\{\Gamma_{mn}(z+t)\} & z<z_0\end{cases} \quad m\neq 0 \\ & +\hat{y}\hat{y}\cdot\cos\left\{\frac{m\pi}{2a}(x+a)\right\}\cos\left\{\frac{m\pi}{2a}(x_0+a)\right\}\sin\left\{\frac{n\pi}{2b}(y+b)\right\} \\ & \times\sin\left\{\frac{n\pi}{2b}(y_0+b)\right\}\begin{cases}\cos\{\Gamma_{mn}(z-t)\}\cos\{\Gamma_{mn}(z_0+t)\} & z>z_0 \\ \cos\{\Gamma_{mn}(z_0-t)\}\cos\{\Gamma_{mn}(z+t)\} & z<z_0\end{cases} n\neq 0 \\ & +\hat{z}\hat{z}\cos\left\{\frac{m\pi}{2a}(x+a)\right\}\cos\left\{\frac{m\pi}{2a}(x_0+a)\right\}\cos\left\{\frac{n\pi}{2b}(y+b)\right\} \\ & \times\cos\left\{\frac{n\pi}{2b}(y_0+b)\right\}\left\{\begin{array}{ll}\sin\{\Gamma_{mn}(z-t)\}\sin\{\Gamma_{mn}(z_0+t)\} & z>z_0 \\ \sin\{\Gamma_{mn}(z_0-t)\}\sin\{\Gamma_{mn}(z+t) & z<z_0\end{array}\right] \\ & \frac{-1}{\Gamma_{mn}\sin\{2\Gamma_{mn}t\}} \end{aligned} \tag{12}$$

In deriving the cavity Greens function series expansion solution is used in transverse plane and closed form solution is used in the direction of propagation.

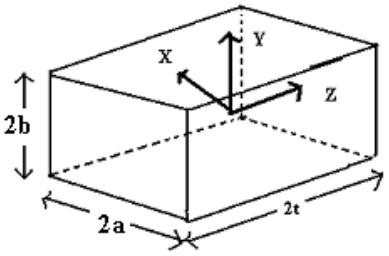

Figure 3. Schematic diagram of a rectangular cavity with its dimension and the axis details.

The electric vector potential $\overline{F}$ in terms of Greens function is given by

$$\overline{F}(r) = \int_{r_0} \tilde{G}(r|r_0) M(r_0) dr_0 \tag{13}$$

With electric vector potential being determined using equations (6), (7), (12) and (13),the scattered field inside the cavity region due to the magnetic currents can be determined from

$$\overline{H} = -j\omega\varepsilon \left[\tilde{I} + \frac{\overline{\nabla\nabla}}{k^2} \cdot \right] \overline{F} \tag{14}$$

The scattered magnetic fields in the waveguide region, due to the presence of the transverse magnetic current densities, are solved from equation (14) by modal expansion approach [27] and is given by

$$H_x^{\text{int}}(M_x) = \sum_m Y_{m0}^e \sin\left\{ \frac{m\pi}{2a}(x+a) \right\} \text{ if } p = m \text{ and } n = 0 \tag{15}$$

The externally radiated field is determined using the spectral domain approach [28] and is given by

$$\begin{aligned} H_x^{ext} &= -\frac{1}{4\pi^2 k\eta} \int_{-\infty}^{+\infty} \int_{-\infty}^{+\infty} \frac{k^2 - k_x^2}{k_z} e^{j(k_x x + k_y y)} dk_x dk_y \\ &\quad \times \iint_{AP} E_y(x', y', 0) e^{-j(k_x x' + k_y y')} dx' dy' \end{aligned} \tag{16}$$

The integration in the spectral domain gives the complex magnetic field distribution of the radiating aperture. The real part is obtained by evaluating the integral for $k_x^2 + k_y^2 \leq k^2$ and the imaginary part

by evaluating the integral for $k_x^2 + k_y^2 \geq k^2$. These two regions correspond to the visible region (radiation field) and the invisible region (evanescent field) and are shown in Figure 4.

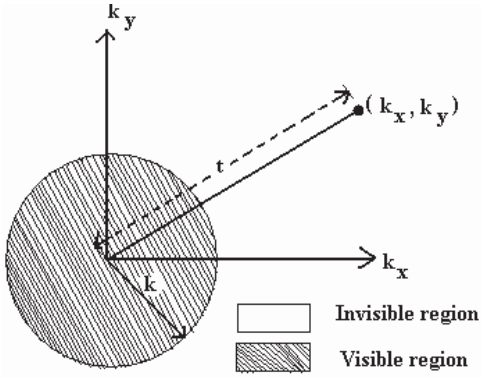

Figure 4. Visible and invisible regions in the spectral domain.

To carry out the integration of equation (16) in the spectral domain the following substitutions are needed.

$$k_x = k \sin\theta \cos\phi \tag{17a}$$
$$k_y = k \sin\theta \sin\phi \tag{17b}$$
$$dk_x dk_y = k^2 \sin\theta \cos\theta d\theta d\phi \quad \text{(In the visible region)} \tag{17c}$$

$$k_x = k \cosh\theta \cos\phi \tag{18a}$$
$$k_y = k \cosh\theta \sin\phi \tag{18b}$$
$$dk_x dk_y = k^2 \sinh\theta \cosh\theta d\theta d\phi \quad \text{(In the invisible region)} \tag{18c}$$

Applying Galerkin's method to the boundary conditions where the same entire domain sinusoidal function is used for testing the expanded magnetic fields, the final form will be a matrix equation of the form

For transmitting mode

$$[L_{11}]\{A^1\} + [L_{12}]\{A^2\} = 2\{L_{inc}\} \tag{19}$$
$$[L_{21}]\{A^1\} + [L_{22}]\{A^2\} = \{0\} \tag{20}$$

For receiving mode

$$[L_{11}]\{A^1\} + [L_{12}]\{A^2\} = \{0\} \tag{21}$$
$$[L_{21}]\{A^1\} + [L_{22}]\{A^2\} = -2\{L_{inc}\} \tag{22}$$

Where

$$L_{11}(p,q) = \iint\limits_{\text{aperture 1}} w_q^1 \cdot \left\{ H_x^{\text{int}} \left(m_{px}^1 \right) + H_x^{cty} \left(m_{px}^1 \right) \right\} dxdy \quad (23a)$$

$$L_{ij}(p,q) = \iint\limits_{\text{aperture i}} w_q^i \cdot H_x^{cty} \left(m_{px}^j \right) dxdy \quad (23b)$$

$$L_{22}(p,q) = \iint\limits_{\text{aperture 2}} w_q^2 \cdot \left\{ H_x^{cty} \left(m_{px}^2 \right) + H_x^{ext} \left(m_{px}^2 \right) \right\} dxdy \quad (23c)$$

$$L_{inc}(i,q) = \iint\limits_{\text{aperture i}} w_q^i \cdot H_x^{inc} dxdy \quad (23d)$$

Solving the matrix equation the basis coefficients can be calculated. The dominant mode reflection coefficient can be calculated as

$$\Gamma = -1 + A_{px}^1 \quad \text{where } p = 1 \quad (24)$$

The received power P_{REC} can be calculated as

$$P_{REC} = \iint\limits_{\text{Aperture}} \vec{E}^{10} \times \left(\vec{H}^{10} \right)^* dxdy \quad (25)$$

Where E^{10} and H^{10} are respectively the electric and magnetic field of the dominant TE_{10} mode in waveguide and is given by

$$H_{x,10}^{\text{int}}(M_x) = Y_0^e \sin \left\{ \frac{\pi}{2a}(x+a) \right\} \quad (26)$$

$$E_{x,10}^{\text{int}}(M_x) = \sin \left\{ \frac{\pi}{2a}(x+a) \right\} \quad (27)$$

Since most measuring devices have an input impedance of 50 Ohms, voltage measured by these is given by

$$V_m = \sqrt{50 \times P_{REC}} \quad \text{Volts.} \quad (28)$$

This is the voltage at the antenna terminals for incident electric field strength 1 volt/meter. The antenna factor is given by the reciprocal of this quantity, i.e.,

$$AF = 1/V_m \quad \text{m}^{-1}. \quad (29)$$

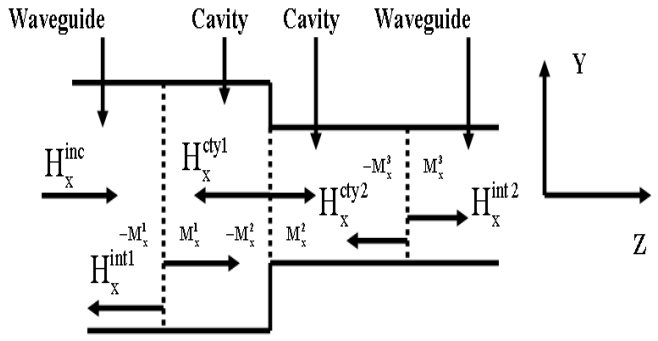

Figure 5. Side view of a waveguide junction.

2.2. Analysis of Waveguide Junction Using MCMT

A side view of a typical waveguide step is shown in Figure 5. From Figure 5 it can be seen that the structure has been modeled with two cavities.

The boundary conditions in aperture 1 (waveguide-cavity), aperture 2 (cavity-cavity) and aperture 3 (cavity-waveguide) are given by

$$H_x^{\text{int}\,1}\left(M_x^1\right)+H_x^{cty\,1}\left(M_x^1\right)-H_x^{cty\,2}\left(M_x^2\right) = 2H_x^{inc} \quad (30a)$$

$$-H_x^{cty\,1}\left(M_x^1\right)+H_x^{cty\,1}\left(M_x^2\right)+H_x^{cty\,2}\left(M_x^2\right)-H_x^{cty\,2}\left(M_x^3\right) = 0 \quad (30b)$$

$$-H_x^{cty\,2}\left(M_x^3\right)+H_x^{cty\,2}\left(M_x^3\right)+H_x^{\text{int}\,2}\left(M_x^3\right) = 0 \quad (30c)$$

The dominant mode reflection coefficient can be calculated using equation (24) whereas dominant mode transmission coefficient can be calculated as

$$T = A_{px}^3 \quad \text{where } p = 1 \quad (31)$$

2.3. Equivalent Network for Thick Interacting Irises Using MCMT

The top view for thick interacting inductive irises is shown in Figure 6.

The equivalent network of the above circuit can be represented as a Pi-network model and is shown in Figure 7, where the series and shunt elements can be represented in terms of reflection coefficient, Γ, and transmission coefficient, T as

$$Y_A = \frac{1-\Gamma+T}{1+\Gamma+T} \quad (32)$$

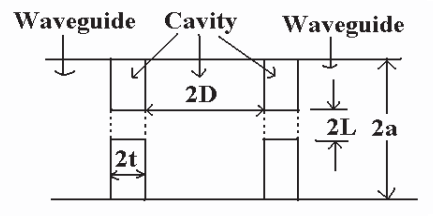

Figure 6. Identical thick interacting inductive irises.

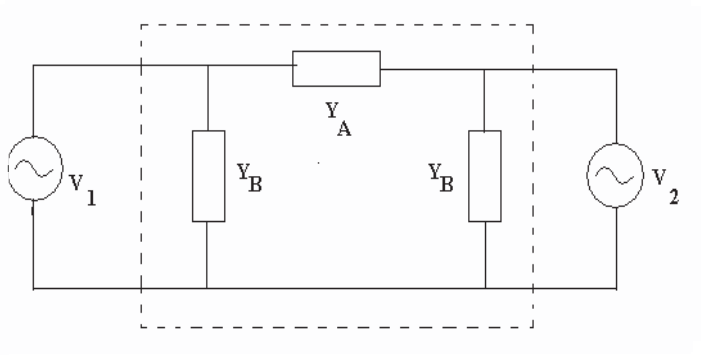

Figure 7. Equivalent Pi-network model of the circuit shown in Figure 6.

$$Y_B = \frac{2T}{(1+\Gamma+T)(1+\Gamma-T)} \tag{33}$$

In terms of Y_A and Y_B, the admittance matrix of the structure $[Y]$ can be expressed as below

$$[Y] = \begin{bmatrix} Y_A + Y_B & -Y_A \\ -Y_A & Y_A + Y_B \end{bmatrix} \tag{34}$$

The eigenvalue or the characteristic value of the matrix $[Y]$ can be calculated by solving the equation

$$|Y - \lambda I| = 0 \tag{35}$$

and is given by

$$\lambda_1 = Y_B \tag{36a}$$

$$\lambda_2 = 2Y_A + Y_B \tag{36b}$$

The eigenvectors or characteristic vectors of the matrix $[Y]$ are the solution of the matrix equation

$$[Y][X] = [\lambda][X] \quad \text{for } [X] \neq [0] \tag{37}$$

and is given by

$$[X_1] = \begin{bmatrix} 1 \\ 1 \end{bmatrix} \tag{38}$$

$$[X_2] = \begin{bmatrix} 1 \\ -1 \end{bmatrix} \tag{39}$$

The eigenvector $[X_1]$ corresponds to even mode excitation or push-push port excitation whereas eigenvector $[X_2]$ corresponds to odd-mode excitation or push-pull port excitation. The equivalent network of the interacting thick inductive irises using push-push port excitation and push-pull port excitation is shown in Figure 8 and in Figure 9, respectively.

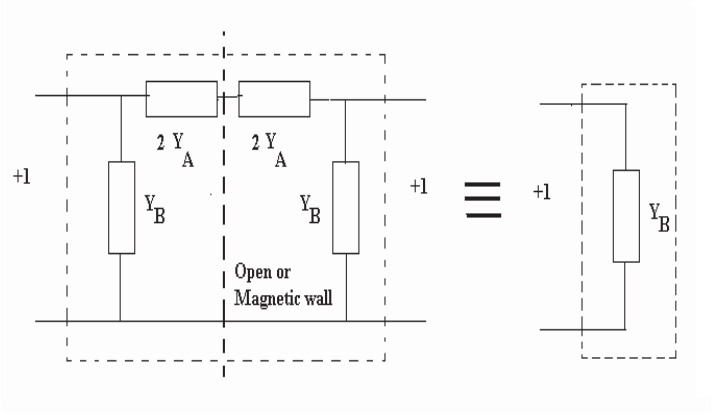

Figure 8. Equivalent network of the interacting thick inductive irises for push-push port excitation.

The push-push port excitation corresponds to magnetic wall symmetry because the magnetic field is zero in the plane of symmetry where as the push-pull port excitation corresponds to electric wall symmetry because the electric field is zero in the plane of symmetry. Due to the existence of the symmetry we only need to consider half of the geometry of the structure because the other half is reflected on the other side of the wall. The cavity model of the structure for push-push or push-pull port excitation is shown in Figure 10.

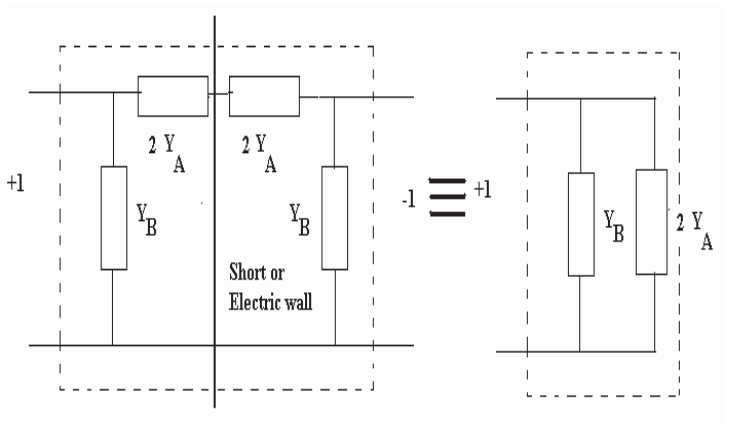

Figure 9. Equivalent network of the interacting thick inductive irises for push-pull port excitation.

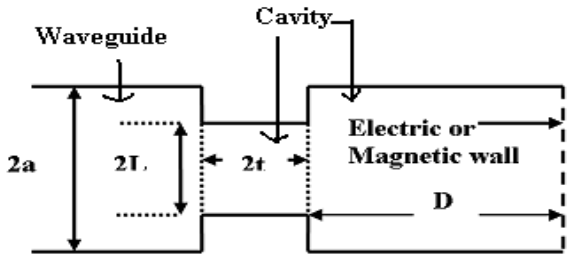

Figure 10. Cavity modeling for the interacting identical thick inductive irises for push-push or push-pull port excitation.

3. NUMERICAL RESULTS

Calculation has been done for the magnitude of reflection coefficient for an open end of a WR-90 waveguide with dielectric plug of thickness 9.51 mm in transmitting mode. The dielectric constant is taken to be the same as that of polystyrene, which is 2.63. The results have been compared with the measured and theoretical data (using stub waveguide technique) available in [1] and are shown in Figure 11. For completeness, the effects of thickness of the dielectric plugs have been studied. To study the effect of varying thickness the graphs available in [1] are reproduced in Figure 12 without comparison (thickness 9.0, 9.5, 10.0, 10.5 and 11.0 mm).

To analyze the open end of a waveguide as a sensor, we have

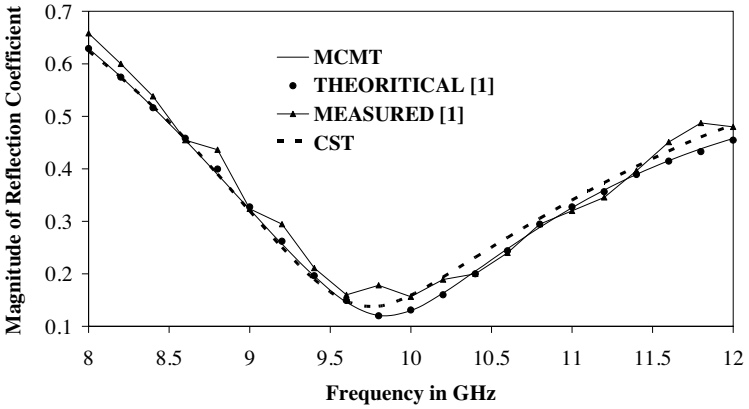

Figure 11. Variation of magnitude of reflection coefficient with frequency for an open ended waveguide radiator with a dielectric plug of thickness $2t = 9.51\,\text{mm}$.

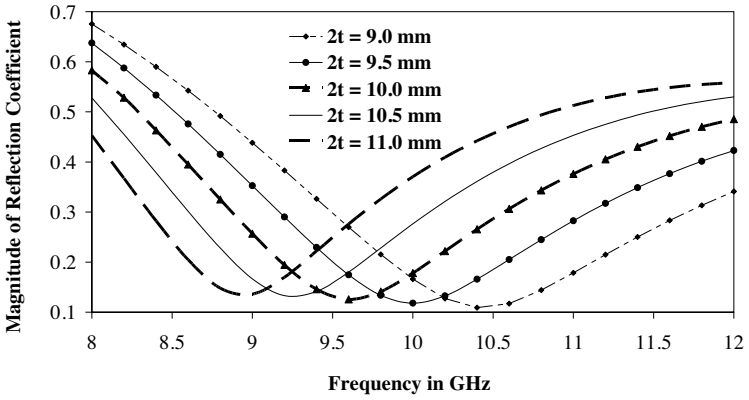

Figure 12. Variation of magnitude of reflection coefficient with frequency for an open ended waveguide radiator with dielectric plug of thickness $2t = 9.0,\ 9.5,\ 10.0,\ 10.5$, and $11.0\,\text{mm}$.

calculated the antenna factor of an open ended waveguide with air dielectric for a WR90 waveguide and compared with measured data. This is shown in Figure 13.

Again for completeness, the effects of thickness of the dielectric plugs with dielectric constant 2.54 have been studied and are shown in Figure 14.

Next, waveguide step junction has been studied and results have

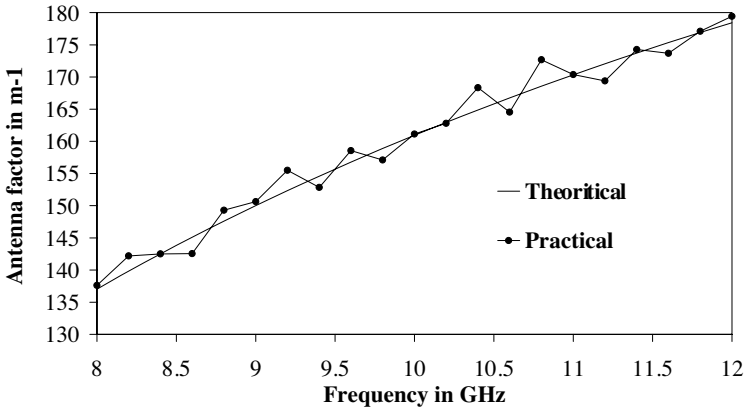

Figure 13. Comparison of MCMT and measured data for antenna factor of an open ended waveguide sensor with air dielectric.

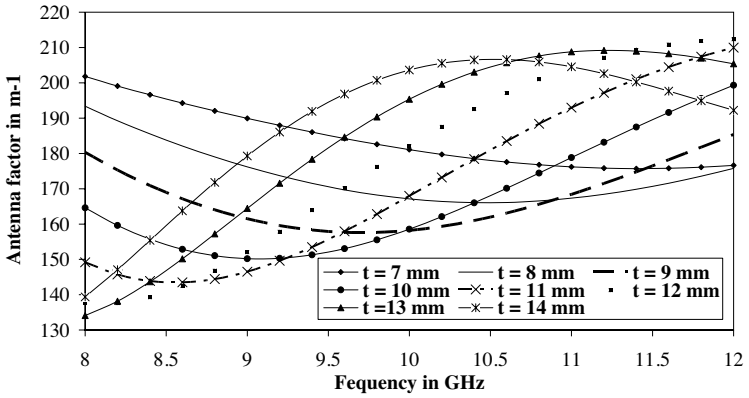

Figure 14. Variation of antenna factor with frequency for an open ended waveguide sensor with a plug for thickness $2t$ = 7, 8, 9, 10, 11, 12, 13 and 14 mm.

been presented and compared with literature available data. The larger rectangular waveguide has dimensions $2a_1 = 2.286$ cm and $2b_1 = 1.0004$ cm and for the smaller one $2a_2 = 1.428$ cm and $2b_2 = 0.65$ cm. The magnitude of reflection coefficients obtained with this method are shown in Figure 15 and compared with [17].

In order to study interaction of two identical thick rectangular inductive irises, the VSWR was computed for the circuit with the following dimensions.

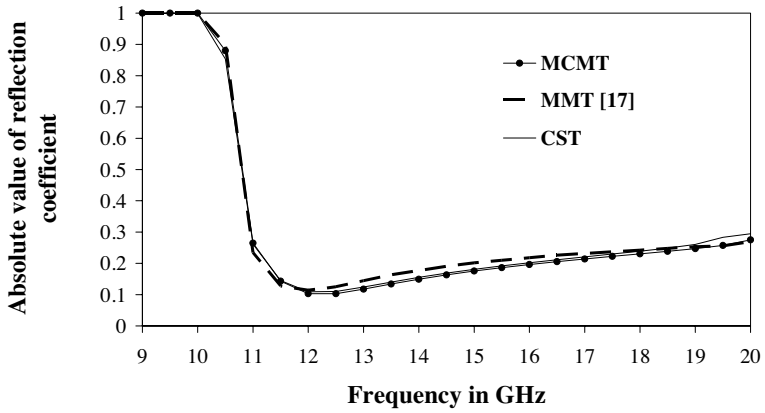

Figure 15. Comparison of magnitude of reflection coefficient obtained from present method and theory in [17] for rectangular-to-rectangular waveguide junction.

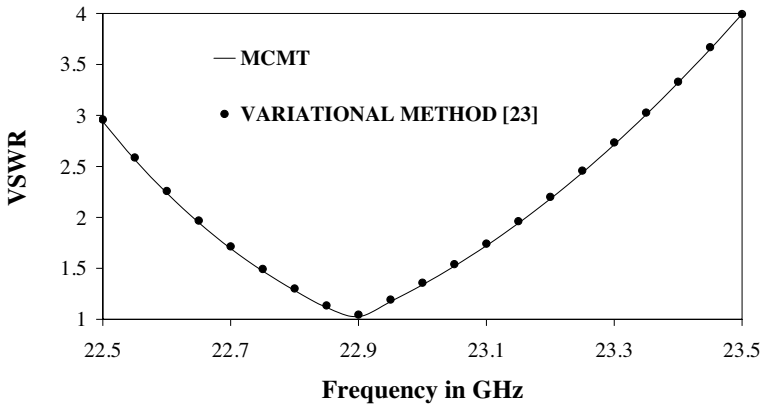

Figure 16. Comparison of VSWR obtained from present method and results in [23] for the circuit shown in Figure 6.

Guide width ($2a$) = 1.067 cm, guide height ($2b$) = 0.432 cm, iris width ($2L$) = 0.452 cm, iris thickness ($2t$) = 0.046 cm, distance between irises ($2D$) = 0.6535 cm in the frequency range 22.5 to 23.5 GHz. The VSWR computed is plotted against frequency in Figure 16 and has been compared with the result obtained in [23]. The resonance is obtained at 22.89 GHz compared with 22.923 GHz in [23].

MCMT data for $|S_{11}|$ have also been compared with measured

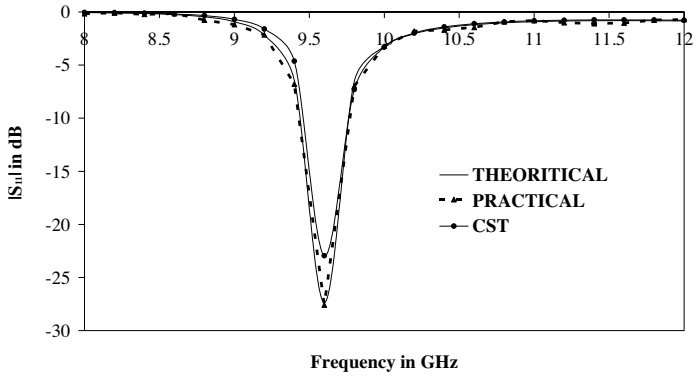

Figure 17. Comparison of $|S_{11}|$ obtained from present method, measurement and CST Microwave Studio simulation for the circuit shown in Figure 6.

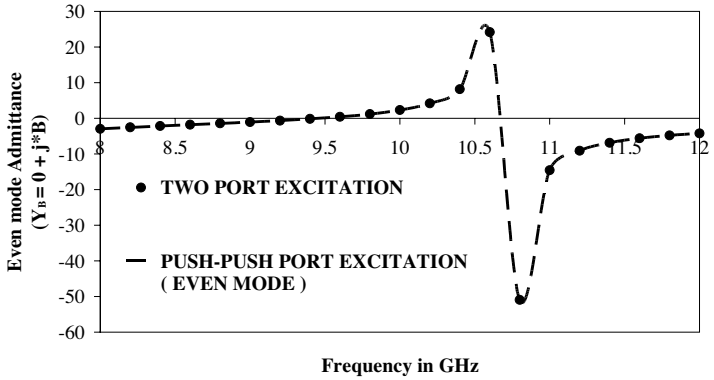

Figure 18. Plot of Y_B (even mode admittance/shunt element in Pi-network representation) for push-push and full two-port excitation.

data and CST simulated data in Figure 17 for the following circuit dimensions.

Guide width $(2a) = 2.286\,\text{cm}$, guide height $(2b) = 1.016\,\text{cm}$, iris width $(2L) = 1.093\,\text{cm}$, iris thickness $(2t) = 0.087\,\text{cm}$, distance between irises $(2D) = 1.647\,\text{cm}$ in the frequency range 8.0 to 12.0 GHz.

The even and odd mode admittances of the circuit with above dimensions have also been calculated for push-push port and push-pull port excitation and have been compared with that obtained with full two port excitation in Figure 18 and Figure 19, respectively.

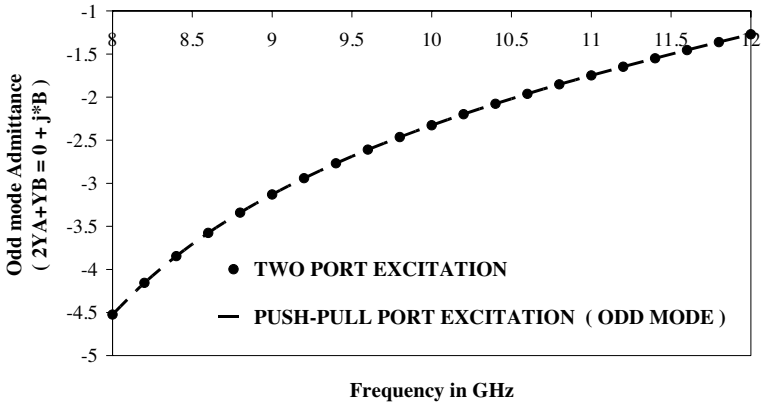

Figure 19. Plot of $(2 * Y_A + Y_B)$ obtained for push-pull and full two-port excitation.

4. CONCLUSION

The MCMT technique has been applied to analyze both the radiator and circuit problems. In the analysis we have considered a total of 3100 modes and $p = 11$ (p is the no of basis function) which are sufficient enough for convergence (However with complexity of the structures these numbers may be changed). With this no. of basis function and modes, the numerical code takes reasonable time to execute in comparison with other commercial electromagnetic softwares or numerical techniques. Though the reflection and transmission coefficients have been calculated for the dominant TE_{10} mode, it should be remembered that during numerical computations we have considered the higher order modes which includes both higher order propagating and evanescent modes. The presence of the higher order modes, in the calculation, effect the aperture electric field distribution and hence the dominant mode reflection or transmission coefficients. Thus the effect of the higher order modes in the equivalent circuit representation of the discontinuity has automatically taken into account. Thus an excellent agreement has been found between the MCMT data, experimental, literature and/or simulation data. The methodology is also very easy to be implemented. Another major advantage of MCMT is that we can directly calculate the reflection, transmission or equivalent network at the discontinuity and so we neither need to add an extra piece of waveguide to define ports nor shifting of reference plane to calculate the equivalent network or S-parameters. Therefore we can conclude the MCMT can be a very

good alternative to other techniques for analyzing radiating as well as non-radiating structures. This also creates the opportunity to dispense with the more costly experimental gathering of the data

Till now all the applications of MCMT have been done for rectangular waveguide based structures in the absence of other materials like ferrites. To use this modeling technique for other types of waveguides like circular or in analyzing waveguide based devices in presence of ferrites materials the expression for the scattered fields in the cavity regions must be modified.

ACKNOWLEDGMENT

This work is supported by Council of Scientific & Industrial Research, India and the authors wish to express their gratitude for this support. The Support provided by Space Technology Cell, Indian Institute of Technology, Kharagpur is also gratefully acknowledged.

REFERENCES

1. Gupta, S., A. Bhattacharyya, and A. Chakraborty, "Analysis of an open-ended waveguide radiator with dielectric plug," *IEE Proc. - Microw. Antennas Propag.*, Vol. 144, No. 2, 126–130, April 1997.
2. Swift, C. T. and D. M. Hatcher, "The input admittance of a rectangular aperture antenna loaded with a dielectric plug," NASA Tech. Note TN-D-4430, April 1968.
3. Swift, C. T., "Admittance of a waveguide-fed aperture loaded with dielectric plug," *IEEE Trans. on Antennas and Propagation*, Vol. 17, No. 3, 356–359, May 1969.
4. Katrich, A. V., N. A. Dumin, and A. O. Dumina, "Radiation of transient fields from the open end of rectangular waveguide," *International Conference on Antenna Theory and Techniques*, 583–586, Sevastopol, Ukraine, September 9–12, 2003.
5. Das, S. and A. Chakrabarty, "Application of multiple cavity modeling technique for accurate analysis of waveguide fed thick rectangular window," *ELECTRO*, 411–414, Varanasi, India, February 3–5, 2005.
6. Das, S. and A. Chakrabarty, "Comparison of an open ended waveguide radiator performance with and without matching stub," *International Conference on Antenna Technology*, 403–405, Ahmedabad, India, February 23–25, 2005.
7. Encinar, J. A. and J. M. Rebollar, "Convergence of numerical solutions of open-ended waveguide by modal analysis and hybrid

modal-spectral techniques," *IEEE Trans. on Microwave Theory and Technique*, Vol. MTT-34, Issue 7, 809–814, July 1986.

8. Baudrand, H., J.-W. Tao, and J. Atechian, "Study of radiating properties of open-ended rectangular waveguides," *IEEE Trans. on Antennas and Propagation*, Vol. 36, No. 8, 1071–1077, August 1988.
9. Zhongxiang, S. and R. H. MacPhie, "A simple method for calculating the reflection coefficient of open-ended waveguides," *IEEE Trans. on Microwave Theory and Techniques*, Vol. 45, No. 4, 546–548, April 1997.
10. Cohen, M. H., T. H. Crowley, and C. A. Levis, "The aperture admittance of a rectangular waveguide radiating into half-space," Rep. 339-22, Contact USAF W33-38-ac-21114, Antenna Lab., Ohio State Univ. Res. Foundation, Columbus, OH, 1951.
11. Das, B. N., "Admittance of rectangular apertures," *Journal of the Institute of Electronics and Telecommunication Engineers*, Vol. 22, No. 3, 133–137, 1976.
12. MacPhie, R. H. and A. I. Zaghloul, "Radiation from a rectangular waveguide with infinite flange-exact solution by the correlation matrix method," *IEEE Trans. on Antennas and Propagation*, Vol. AP-28, 497–503, July 1980.
13. Gupta, S., "Electromagnetic field estimation in aperture and slot antennas with their equivalent network representation," Ph.D. Dissertation, Department of Electronics and Electrical Communication Engineering, Indian Institute of Technology, Kharagpur, India 1996.
14. Eleftheriades, G. V., A. S. Omar, L. P. B. Katehi, and G. M. Rebeiz, "Some important properties of waveguide junction generalized scattering matrices in the context of the mode matching technique," *IEEE Trans. of Microwave Theory and Techniques*, Vol. 42, No. 10, 1896–1903, October 1994.
15. Mongiardo, M., P. Russer, M. Dionigi, and L. B. Felsen, "Waveguide step discontinuities revisited by the generalized network formulation," *Microwave Symposium Digest, 1998 IEEE MTT-S International Volume 2*, June 7–12, 1998.
16. Chen, C., K. Choi, H. K. Jung, and S. Y. Hahn, "Analysis of waveguide discontinuities in H-plane using finite element-boundary element technique," *IEEE Trans. Of Magnetics*, Vol. 30, No. 5, 3168–3171, September 1994.
17. Lin, S. L., L. W. Li, T. S. Yeo, and M. S. Leong, " Novel unified mode matching analysis of concentric waveguide junctions," *IEEE Trans. on Antennas and Propagation*, Vol. 148, No. 6, 369–374,

December 2001.

18. Wexler, A., "Solution of waveguide discontinuities by modal analysis," *IEEE Trans. Microw. Theory Tech.*, Vol. MTT-15, No. 9, 508–517, September 1967.
19. Levy, R., "Derivation of equivalent circuits of microwave structures using numerical techniques," *IEEE Trans. Microw. Theory Tech.*, Vol. 47, No. 9, 1688–1695, September 1999.
20. Guglielmi, M. and C. Newport, "Rigorous, multimode equivalent network representation of inductive discontinuities," *IEEE Trans. Microw. Theory Tech.*, Vol. 38, No. 11, 1651–1659, November 1990.
21. Palais, J. C., "A complete solution of the inductive iris with TE_{10} incidence in rectangular waveguide," *IEEE Trans. of Microwave Theory and Techniques*, Vol. 15, 156–160, March 1967.
22. Rozzi, T. E., "Equivalent network for interacting thick inductive irises," *IEEE Trans. on Antennas and Propagation*, Vol. 20, No. 5, 323–330, May 1972.
23. Rozzi, T. E., "The variational treatment of thick interacting inductive irises," *IEEE Trans. on Antennas and Propagation*, Vol. 21, No. 2, 82–88, February 1973.
24. Collin, R. E., "Variational methods for waveguide discontinuities," *Field Theory of Guided Waves*, Chapter 8, McGraw-Hill Book Company, New York 1960.
25. Harrigton, R. F., "Deterministic problems," *Field Computation by Method of Moments*, First edition, Chapter 1, Section 1.3, 5–9, Roger E. Krieger Publishing Company, INC., Malabar, Florida, USA, 1968.
26. Mittra, R., T. Itoh, and T.-S. Li, "Analytical and numerical studies of the relative convergence phenomenon arising in the solution of an integral equation by the moment method," *IEEE Trans. Microw. Theory Tech.*, Vol. MTT-20, No. 2, 96–104, February 1972.
27. Harrigton, R. F, "Microwave network," *Time Harmonic Electromagnetic Fields*, First edition, Chapter 8, Section 8-2, 389–391, McGraw-Hill Book Company, New York, USA, 1961.
28. Chakrabarty, A., "Synthesis of phase function for a desired radiation pattern and fixed amplitude distribution," Ph.D. Dissertation, Department of Electronics and Electrical Communication Engineering, Indian Institute of Technology, Kharagpur, India 1981.